

Investigation and simulation of hot forming of alumina based materials

A. BATAILLE*, J. CRAMPON

Laboratoire de Structure et Propriétés de l'Etat Solide, U.M.R. CNRS 8008, Université des Sciences et Technologies de Lille, F-59 655 Villeneuve d'Ascq Cedex, France

E-mail: alain.bataille@univ-lille1.fr

Hot forming of a MgO-doped alumina and of a alumina-based nanocomposite has been carried out at 1400°C under vacuum. The forming consisted of discs of the materials being punched between graphite parts into hemispheres. The loading data are presented along with a simulation of these data. The MgO-doped alumina disc broke before completion of the test, whereas the alumina based nanocomposite disc was formed into a hemisphere with reduced damage. Calculated loading data fitted monitored loading data satisfactorily. Microstructural investigations were performed on the nanocomposite hemisphere. The microstructural damage consisted of reduced cavitation which occurred essentially in a shallow region of the outer surface of the hemisphere. The reduced damage observed on the nanocomposite microstructure must be associated with the fineness of the microstructure and the reduced alumina grain growth in this material. Considering the severity of this forming process in terms of deformation, this test illustrates very well the superplasticity of the nanocomposite material. These observations confirmed results gathered from compressive testing. © 2003 Kluwer Academic Publishers

1. Introduction

High temperature shaping of ceramic materials has been investigated for a long time and studies are continuously reported by different authors [1–12]. Studies of the hot forming of alumina or alumina-based ceramics are rare and investigations of the plastic deformation of these materials reveal the crucial importance of microstructural control during deformation. Indeed, for example, hot-forming of zirconia ceramics has been more extensively demonstrated due to lower microstructural evolution during deformation. Alumina however exhibits important dynamic grain growth, which is deleterious for further deformation capabilities.

Superplastic deformation of fine grained aluminas is a boundary diffusion process, involving mainly grain boundary sliding. Also, cavitation may become an important accompanying process for deformation when the mean grain size is over a few micrometers. From this basis, one of the necessary conditions for dense alumina to exhibit important deformation capabilities is to start with a submicrometre microstructure. The finer the initial microstructure, the better the plastic behaviour.

The present paper reports on the hot-forming of an alumina-based nanocomposite. The results are compared with those of a MgO-doped alumina. The nanocomposite compressive deformation behaviour has been presented previously [2]. This deformation

behaviour proved to be superplastic in the conditions corresponding to the study in terms of temperature, true stress and strain rate. One may argue that superplasticity must be investigated under tension to be proven. Here the authors decided to investigate the formability of the two materials under a much more severe testing method consisting of punching a flat disc into a hemisphere. The loading data are presented along with a simplified simulation of the monitored parameters, based on an analysis by Wu *et al.* [1].

2. Experimental procedure

The nanocomposite material consists of a fine and homogeneous distribution of carbon nanoparticles in an alumina matrix. The alumina matrix was doped with 500 ppm MgO. The size of the particles and of the alumina grains were in the range of 20 to 50 nm and 650 nm respectively. The carbon content was about 1.2 wt%.

The alumina material was MgO-doped, with a mean grain size of 1200 nm. Both materials were prepared by hot pressing alumina powders¹. Details of both material preparation and characterisation have been reported previously [2]. The densities were higher than 99% of theoretical. The compressive deformation investigations of the nanocomposite and of the alumina led to two constitutive equations which are

*Author to whom all correspondence should be addressed.

¹Baikowski, SM8.

respectively:

$$\dot{\varepsilon} = C_1 \cdot \sigma^{2.4} \cdot d^{1.6} \cdot \exp\left(-\frac{515,000}{RT}\right) \quad (1)$$

$$\dot{\varepsilon} = C_2 \cdot \sigma^{1.6} \cdot d^{2.35} \cdot \exp\left(-\frac{560,000}{RT}\right) \quad (2)$$

where $\dot{\varepsilon}$ is the true strain rate in s^{-1} , σ is the true stress in MPa, d is the grain size, T is the temperature, R is the gas constant and C_1 and C_2 are constants. The activation energies are given in kJ/mol.

Taking into account the initial grain sizes, these equations have been reformulated and computed at $T = 1400^\circ\text{C}$, to give Equations 3 and 4 for the nanocomposite and for the alumina, respectively

$$\sigma = 900 \cdot \dot{\varepsilon}^{0.42} \quad (3)$$

$$\sigma = 11,100 \cdot \dot{\varepsilon}^{0.62} \quad (4)$$

The true stress is in MPa when the true strain rate is in s^{-1} in these equations. These equations do not consider the grain growth that can occur during deformation at high temperature.

Regarding the hot-forming tests, flat circular disks were ground and diamond-polished to a thickness of 2.2 mm for a diameter of 30 mm. These discs were placed between a hemispherical punch and a circular die, made out of nuclear grade graphite². The punch diameter was 17 mm and the die inner diameter was 20 mm. Disc edges were by not clamped during testing. Following heating at $10^\circ\text{C}/\text{min}$ up to 1400°C under secondary vacuum, the discs were punched at a constant displacement speed of 0.12 mm/min. A typical forming time was a hour.

3. Results and discussions

Forming data are plotted in Fig. 1 for both the nanocomposite and the alumina. Forming loads are correspondingly higher for the latter. This must be associated with

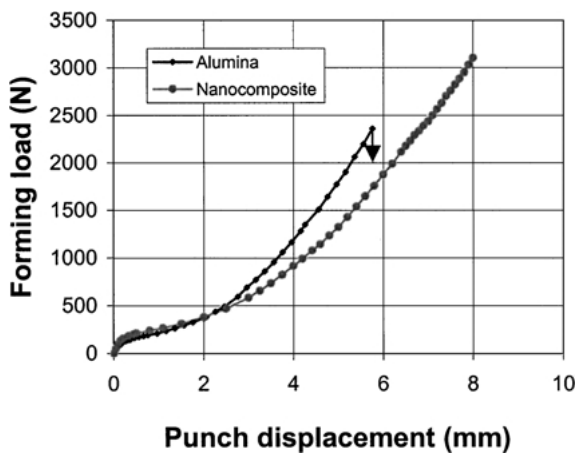


Figure 1 Forming load versus punch displacement for both alumina and nanocomposite materials at punch velocity $v = 1.2 \times 10^{-1} \text{ mm}/\text{min}^{-1}$ and at $T = 1400^\circ\text{C}$.

²Carbone lorraine, high quality graphite 2114.

the higher initial grain size resulting in a higher flow stress. Higher flow stresses have also been reported for deformation tests on the alumina material [2].

The alumina disc broke before completion of the test, whereas, the nanocomposite underwent no rupture. Fig. 2 shows the discs after forming. According to Wu *et al.* [1], the disc underwent large biaxial tensile stretching during forming. These authors discussed the severity of this test in deformation terms and concluded this process is much more severe than uniaxial tension.

From Wu's paper, the geometrical analysis of the disc being formed between the punch and the die resulted in two equations. These expressed the growing surface 'S' of the deformed portion of the disc and the punch displacement 'd' as follows:

$$S = \Pi \cdot (a^2 - R^2 \cdot \sin^2(\beta)) / \cos(\beta) + 2\Pi R^2(1 - \cos(\beta)) \quad (5)$$

$$d = R \cdot (1 - \cos(\beta) - \text{tg}(\beta) \cdot \sin(\beta)) + a \text{tg}(\beta) \quad (6)$$

where 'R' and 'a' are respectively the punch radius and the die inner radius, and β is the angle from the center of the punch to the contact points (see schematic diagram in Fig. 3).

Here, the strain is defined as the variation of disc surface relative to the initial one. The true strain is the natural logarithm of the ratio of current surface S to initial one. The true strain rate is determined from this knowledge. True strains and true strain rates were computed using Equations 5 and 6 for the presented geometry of the equipment with a punch velocity of 0.12 mm/min. Results are shown in Fig. 4.

Both true strain and true strain rate only depend on the geometrical analysis and on the growing surface 'S'. It can be noted that the strain rate is not constant and that a maximum of $\dot{\varepsilon} = 1.8 \times 10^{-4} \text{ s}^{-1}$ is reached close to the completion of the test, i.e., when the punch displacement is larger than 8 mm. The arithmetic mean true strain rate values are $\dot{\varepsilon} = 1 \times 10^{-4} \text{ s}^{-1}$ for the nanocomposite and $\dot{\varepsilon} = 7.7 \times 10^{-5} \text{ s}^{-1}$ for the alumina. The true strain reaches a value of $\varepsilon = 0.45$ for the nanocomposite when the test was completed and a value of about $\varepsilon = 0.25$ for the alumina when the disc broke.

Also the evolution of the load with punch displacement was simulated from the knowledge of the simplified stress analysis proposed by Wu *et al.* [1]. On the basis of the mean true strain rates determined for both materials, true stresses were computed from Equations 3 and 4. Taking into account the growing surface 'S' of the deformed disc, the forming load evolution was computed and the corresponding data are presented in Fig. 5. The fitting shows good agreement with the experimental curve of Fig. 1. The underestimate of the computed data corresponding to the first two millimetres of punching displacement is associated (i) with the elastic loading, which has not been taken into account and (ii) with the setting of the test with the elastic loading. Also, the fitting suggests that grain growth is not dominant in the loading determination

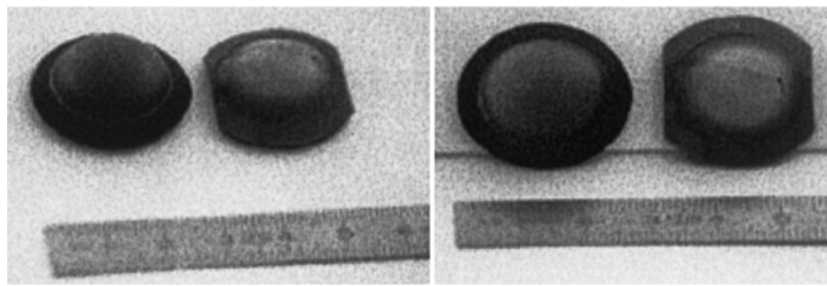


Figure 2 Side view (a) and Top view (b) of the formed discs. The nanocomposite is black-coloured and is placed on the left hand side of photographs and the alumina is grey-coloured, and is on the right hand side of photographs.

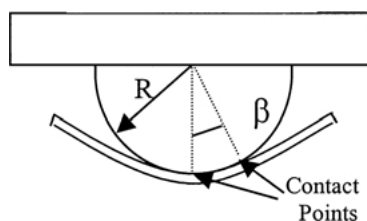


Figure 3 Schematic diagram of the punch and formed disc.

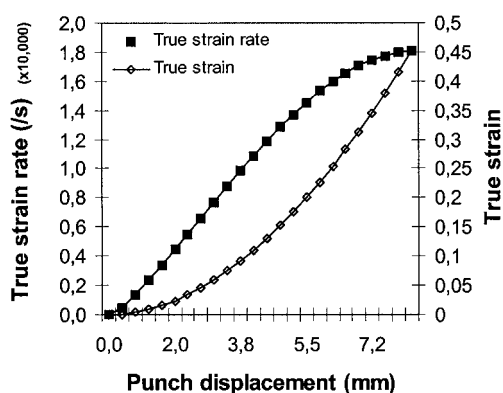


Figure 4 Computation of the true strain and true strain rates versus punch displacement.

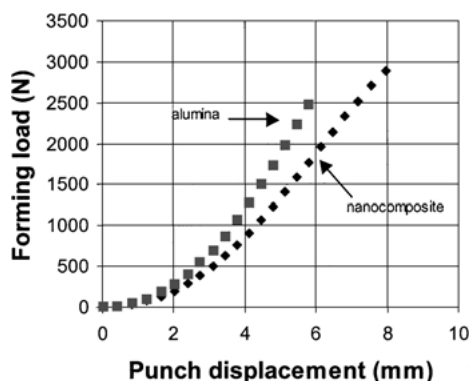


Figure 5 Simulation of the evolution of forming load versus punch displacement for both materials for a true strain rate of $1 \times 10^{-4} \text{ s}^{-1}$.

during the test, for the present testing conditions. Basically the flow stresses were calculated from results obtained by compressive testing. The good fit obtained between experimental and computed loading led to the conclusion that similar values are appropriate for flow stresses under compressive loading or tensile loading. Plastic deformation under tensile loading is to be carried out to confirm that this is the case.

The observation of the microstructure revealed some cavitation located on the outer surface of both deformed discs.

For the alumina disc, the fracture, which is clear from Fig. 2, must be associated with the linkage of cavities. For this disc, cavitation occurred earlier in the test, due to the higher initial grain size and this resulted in the failure, which occurred abruptly and resulted in a sudden load drop. From previous work on compressive deformation [2], the microstructure evolution of the alumina material has been observed to be more active in terms of cavitation and grain growth. Indeed, at a true compressive strain of $\epsilon = -0.30$, the grain growth corresponded to an increase of 110%, i.e., a grain size of 2.62 micrometers. This important grain growth resulted in the development of cavitation. In association with the more severe strain conditions of the present work, such a behaviour explains the early failure of the alumina disc.

Such a relationship between grain size and cavitation has been observed and presented for a variety of ceramic materials [2, 13, 14].

As for the nanocomposite material, the grain growth was reduced due to the presence of the carbon particles. As a result little cavitation occurred under the forming conditions and no linkage of cavities was observed. Scanning electron microscopy observations of a section of the formed nanocomposite disc showed cavities with sizes comparable to the grain size. Figs 6 and 7 show the limited cavitation of the nanocomposite microstructure.

Cavitation was mainly located within a layer of about a hundred micrometers from the outer surface and mainly around the apex area. Moreover no preferential orientation of the cavities was revealed. These microstructural changes are not associated with a boundary glassy phase as previous studies of the materials have not revealed the presence of such a glassy phase. The limited cavitation observed in the nanocomposite microstructure emphasizes the strength of the alumina grain boundaries in the absence of any liquid phase. For the nanocomposite material the final mean grain size was slightly higher than one micrometer in the apex area. It remained submicrometric away from this area. Moreover the grain shape remained equiaxed, which suggests strongly that grain position exchanges have taken the main part in its deformation.

Some authors have reported on the forming of Y-TPZ [14] and concluded that a combination of fine porosity and fine grain size is beneficial. Small cavities can ease material deformation when associated with a fine

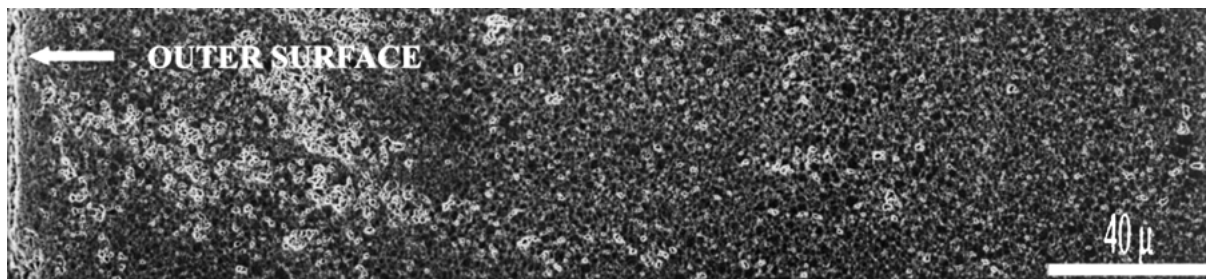


Figure 6 Low magnification SEM micrograph of nanocomposite microstructure showing restricted cavitation in the apex area of the formed disc.

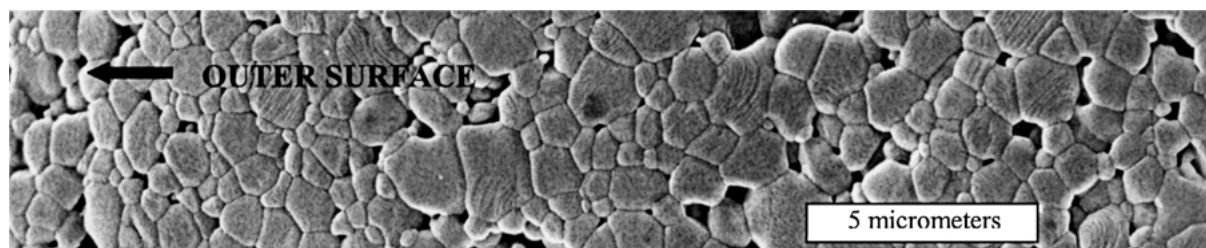


Figure 7 SEM micrograph of nanocomposite showing fine-grained microstructure in the apex area of the formed disc.

microstructure. Here, it is proposed that deformation must be mainly associated with grain boundary sliding through a diffusive process. However cavitation may have contributed to some extent to the forming of the nanocomposite disc.

On the contrary cavitation has proved to be dominant and very damaging for the alumina material. The micrometric grain size in the MgO-doped alumina resulted in the accommodation of the deformation both by grain boundary sliding and by cavitation. Indeed grain boundary sliding must have been too slow to accommodate all the deformation on its own. Hence cavitation took place and must have dominated the deformation accommodation up to the failure of the alumina disc.

Cavitation phenomena are difficult to avoid totally in ceramics [5]. However, cavities remained closed for the nanocomposite material up to the end of the test and these could have been easily healed by a subsequent heat treatment.

4. Conclusion

Punch stretching formability of alumina based material has been improved by the use of finer initial grain sizes, and the reduction of grain growth associated with homogeneously distributed carbon nanoparticles. The coarsening of microstructure in alumina material results in cavitation and subsequent fracture of the formed part.

In reference to the severity of the stretching test in terms of tensile deformation, the nanocomposite exhibited a large ductility which illustrated very well its superplasticity.

The agreement between calculated data and measured ones suggests some similarity between flow stresses under compressive deformation and under tensile deformation for the testing conditions and materials studied.

Forming parameters have still to be optimised in terms of time taken with reference to compression

testing carried out with the nanocomposite material, for which a true strain rate of $\dot{\epsilon} = 10^{-3} \text{ s}^{-1}$ has been reached without microstructural cavitation and with little grain growth.

Acknowledgements

This work was partially supported by the county of "Nord-Pas de Calais," France and by the FEDER, "Fond Européen de Développement Economique et Régional."

References

1. X. WU and I. W. CHEN, *J. Amer. Ceram. Soc.* **73**(3) (1990) 746.
2. A. BATAILLE, J. CRAMPON and R. DUCLOS, *Ceram. Int.* **25** (1999) 215.
3. P. F. BECHER, *J. Amer. Ceram. Soc.* **56**(11) (1977) 1015.
4. E. A. MAGUIRE and R. L. GENTILMAN, *ibid.* **60**(2) (1981) 255.
5. C. CARRY and A. MOCELLIN, in Proceedings of the International Conference on Superplasticity, Grenoble, Sept. 1985, edited by B. Baudalet and M. Suery, p. 16.1.
6. B. J. KELETT and F. F. LANGE, *J. Amer. Ceram. Soc.* **69**(8) (1986) C172.
7. P. C. PANDA, J. WANG and R. RAJ, *ibid.* **71**(12) (1988) C507.
8. J. WITTENAUER, T. G. NIEH and J. WADSWORTH, *Scripta Met. Mat.* **26** (1992) 551.
9. S. L. HWANG and I. W. CHEN, *J. Amer. Ceram. Soc.* **77**(10) (1994) 2575.
10. O. KWON, C. SCOTT NORDHALL and G. L. MESSING, *ibid.* **78**(2) (1995) 491.
11. T. ROUXEL and J. L. BESSON, *J. Eur. Ceram. Soc.* **17** (1997) 1963.
12. D. M. OWEN and A. H. CHOKSHI, *Acta Mater.* **46**(2) (1998) 719.
13. F. BECLIN, PhD thesis, University of Lille, 1995.
14. I. A. AKMOULIN, M. DJAHAZI and J. J. JONAS, in Proceedings of the International Conference on Superplasticity in Advanced Materials, edited by S. Hori, M. Tokizane and N. Furushiro (Japan Soc. For Research on Superplast., 1991) p. 186.

Received 18 September 2002
and accepted 20 May 2003